ACS Sustainable Chemistry & Engineering

pubs.acs.org/journal/ascecg

Research Article

Drinking Water Electrochlorination in a Single-Pass Biomimetic Flow Cell with Zero Salt Dosing

Inmaculada García-López,* Luis Fernando Arenas, Jonas Hereijgers, Vicente Ismael Águeda, and Amalio Garrido-Escudero

Cite This: *ACS Sustainable Chem. Eng.* 2024, 12, 3130−3141

Read Online

ACCESS | Metrics & More | Article Recommendations | Supporting Information

ABSTRACT: Electrochlorination is an efficient and cost-effective treatment technique to provide safe drinking water in remote locations. Commercial electrochlorinators normally rely on the replenishment of salts to generate the disinfectant. In this work, a novel undivided electrochemical flow cell with affordable electrode materials (graphite and stainless steel) is proposed, simulating the chlorides naturally present in groundwater sources (25−250 mg·L^{-1}). The biomimetic 3D-printed flow field allows to generate chlorine in a single pass with residence times lower than 1 min. Parameters controlling the electrochlorination are evaluated through a definitive screening design and include applied current, flow rate, and concentration of ions, such as chloride, sulfate, bicarbonate, and calcium. The main factors influencing free chlorine are chloride concentration, applied current, and water inlet flow rate. These significant parameters are further studied and optimized in a Box−Behnken design, obtaining free chlorine concentrations higher than 0.5 mg·L^{-1} in all evaluated chloride concentrations, with a maximum of 3.70 mg·L^{-1} for the most favorable conditions. The optimal conditions for achieving the minimum specific energy consumption (SEC) while maximizing chlorine production were identified at a chloride concentration of 250 mg·L^{-1}, operating with a flow rate of 400 mL·h^{-1} and applying a current of 35.5 mA. This setup resulted in the lowest observed SEC of 0.59 Wh·mg FC^{-1}. The favorable results for electrochlorination in this type of cell open up the possibility for scale-up, allowing processing at higher drinking water flow rates.

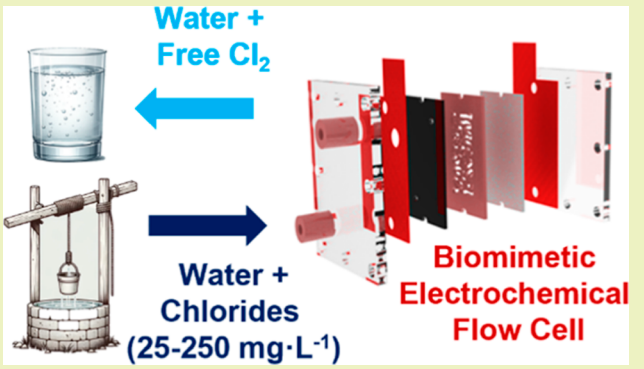

KEYWORDS: *3D printing, electrochemical water treatment, differential growth, free chlorine, nature-inspired, water disinfection*

1. INTRODUCTION

Access to clean and safe drinking water is a fundamental human right, and it is a crucial component for the socioeconomic development of a community. However, the lack of clean drinking water in developing countries remains a significant problem, especially in rural areas, due to inadequate infrastructure, missing technical skills, or a lack of access to chemical products and electricity.[1,2] Although diseases like cholera, dysentery, typhoid, and polio can be spread by polluted drinking water, it is presently estimated that over 2 billion people consume polluted water, which results in about 485,000 fatalities yearly from diarrhea alone.[3,4]

Point-of-use (POU) treatment techniques are frequently examined as alternatives in areas where centralized drinking water treatment is difficult to implement. These have been demonstrated to be effective at removing microorganisms and have successfully reduced diarrhea occurrences.[5−7] Among the most widespread POU treatments, chlorine has long been a preferred disinfectant for water disinfection because it eliminates a wide spectrum of waterborne pathogens at low operating costs.[8−10] Besides, chlorination guarantees effectiveness in both primary and secondary disinfection, removing microorganisms not only at the point of treatment but also during water delivery to the point of use. However, conventional chlorination also has some drawbacks, such as the handling of concentrated hypochlorite solutions or the need for a chemical supply chain.[10,11] The latter can be particularly problematic in some developing countries or during emergency situations because the distribution network for bulk chemical commodities can be unreliable while access to remote locations is often difficult.[6,12]

Electrochlorination has been implemented in recent decades because of its benefits over traditional chlorination as the chlorine can be generated on-site. This reduces the reliance of the system on transportation and storage, boosting its

Received: October 29, 2023
Revised: January 24, 2024
Accepted: January 26, 2024
Published: February 14, 2024

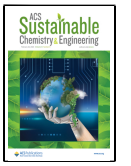

flexibility and adaptability,[13] and contributes to the sustainability of the water treatment process. Moreover, electrochlorination can maintain residual disinfection in stored water, and the amount of disinfectant produced can be adjusted according to the on-site demand, making this mode of disinfection easier to operate.[14] Besides, recent studies revealed an increased inactivation efficiency of in situ electrochlorination over conventional chlorination.[15]

To generate chlorine electrochemically, an electric current must be applied to the electrodes in a chloride-containing solution by using divided or undivided flow reactors. The applied electricity may be provided from renewable sources, such as solar or wind, making this technology even more sustainable and portable.[16,17] The main reactions that take place during the electrochlorination process are described in eqs. 1−4.[18,19] The term "free chlorine (FC)" refers to the sum of solvated chlorine gas (Cl_2), hypochlorous acid (HOCl), and hypochlorite ion (OCl^-).[20] According to the speciation diagram,[21] the equilibrium between Cl_2−HOCl−OCl^- is governed by the pH of the solution. By analyzing the pH level, it is possible to theoretically determine the concentration ratios of all three species for any specific pH of the solution.

Anode

$$2Cl^- \rightarrow Cl_2 + 2e^- (E^\circ = +1.36\ V \text{ vs SHE}) \quad (1)$$

Bulk

$$Cl_2 + H_2O \rightarrow H^+ + Cl^- + HOCl \quad (2)$$

$$HOCl \leftrightarrows OCl^- + H^+ (pK_a = 7.5 \text{ at } 25^\circ C) \quad (3)$$

Cathode

$$2H_2O + 2e^- \rightarrow 2OH^- + H_2 (E^\circ = -0.83\ V \text{ vs SHE}) \quad (4)$$

The electrochemical production of active chlorine involves several factors, such as the kind of electrochemical reactor used (whether it is a divided or undivided cell, the distance between electrodes, etc.), the type of anode material, the operational conditions such as temperature and pH, the applied current or potential, the flow rate and fluid dynamics, as well as the chloride concentration.[22] The material used for the anode plays a crucial role in determining the efficiency of active chlorine generation and avoiding unwanted reactions such as oxygen evolution. Anodes made from iridium and ruthenium oxides, known as active anodes, generally yield better results in producing active chlorine than nonactive anodes made from materials like tin dioxide and lead dioxide.[23] Previous studies with these types of anodes reported levelized costs (LC) of water treatment of 0.815 $\$\cdot m^{-3}$ for the electrochemical system (grid connected) and 0.777 $\$\cdot m^{-3}$ for the system supplied by solar panels versus 0.789 $\$\cdot m^{-3}$ for the chemical system for a chlorine dose of 1.75 $mg\cdot L^{-1}$.[15] The LC for the electrochemical and chemical systems is very close to their application, depending more on convenience. Graphite is, however, a cost-effective choice for electrochlorination in the least developed countries due to its affordability and accessibility compared to more efficient yet expensive anode materials and its reduced probability of generating more toxic, highly oxidized chlorine compounds. Its lower cost makes the initial setup and maintenance of electrochlorination systems more financially feasible, ensuring accessibility and sustainability of water treatment solutions in resource-limited settings. The capital expenditure associated with the graphite-based system was estimated at 224 $,[24] in contrast to 500 $ of an electrochlorinator comprising Ti/RuO_2 anodes,[15] despite the fact that the processing capability of the former is an order of magnitude higher.

Most commercial electrochlorinators require high concentrations of chloride ions to produce concentrated streams of hypochlorite.[11,25] Users need to replenish NaCl, preferably of high purity, to avoid side reactions. This may imply barriers to adoption of the technology and long-term use abandonment due to the requirement of consumables.[26] However, most water sources naturally contain chloride ions, although their concentration varies significantly according to the location within a typical range of 10 to 250 $mg\cdot L^{-1}$. Because the reaction efficiency declines at low ionic and chloride concentrations, more energy is required under these conditions, and the operating electrode potentials are higher. The implementation of electrochemical flow cells is a known method for increasing the efficiency at low reagent concentrations. By decreasing the interelectrode gap, the cell resistance is reduced and the electrolyte velocity is augmented. The latter results in enhanced mass transfer to and from the electrodes, while the faster mixing of the reactants accelerates the rate of the homogeneous reaction steps, enhancing the conversion of reactants into products.[27] Furthermore, flow reactors provide increased control over the treatment process,[28] which makes it simpler to maintain a steady water quality.

In this study, a novel undivided, filter-press-type electrochlorinator based on a biomimetic flow field is proposed. Indeed, the geometry of the flow field has a strong influence on the mass-transfer performance of a flow cell and therefore its productivity and energy use.[29] The main novelty of this work lies in the application of biomimetic differential growth patterns[30,31] to an electrochlorination system operating at low chloride concentrations. This biomimetic flow field design was developed in our previous work,[32,33] where it demonstrated improvement in the overall electrochemical mass-transfer performance in electrochemical flow cells by increasing radial mixing[32] while maintaining an overall plug flow behavior. The pressure drop was measured and found to be similar to typical values for laboratory electrochemical cells and was therefore manageable.[33] Moreover, the total conversion in flow reactors depends on the length of the electrode channel, which is another advantage of the biomimetic geometry as a long channel can be folded into a small surface. As the adoption of these types of devices can be affected by the cost of the system, the tested electrode materials were inexpensive graphite and stainless-steel. This electrochemical reactor operates in single-pass mode and is intended for low chloride concentrations for on-site, domestic, emergency, or portable applications.[34,35] The manufacture of the intricate biomimetic flow field is enabled by fast prototyping by using accessible resin stereolithography (SLA) 3D printing.

The experiments were performed according to the design of experiments (DOE) methodology.[36] This allows us to plan, conduct, and analyze experiments to obtain the maximum information on a system with the minimum number of runs. This was preceded by using definitive screening design (DSD) to select the parameters that have the largest influence on FC generation.[37] Once these variables were selected, an optimization study was carried out with response surface optimization, specifically the Box−Behnken design.[38]

https://doi.org/10.1021/acssuschemeng.3c07066
ACS Sustainable Chem. Eng. 2024, 12, 3130−3141

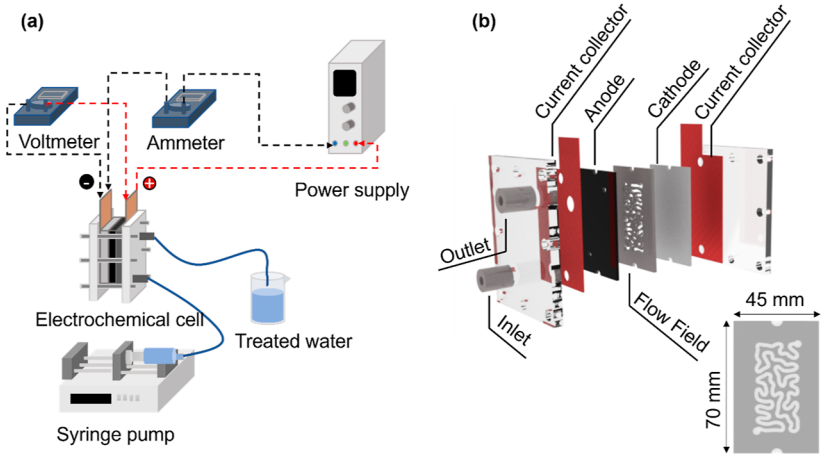

Figure 1. Experimental arrangement. (a) Flow system and instrumentation. (b) Electrochemical flow cell assembly.

2. MATERIALS AND METHODS

2.1. Reagents and Analysis. The electrolyte for each experiment was prepared by diluting NaCl into distilled water to obtain variable chloride concentrations, simulating typical compositions in groundwater. The influence of the presence of various other ions in water on electrochlorination was also investigated. The substances used in this study, including NaCl, Na_2SO_4, $NaHCO_3$, and $Ca(OH)_2$, were reagent grade (Sigma-Aldrich, Germany) and used with no further purification. It was confirmed that the initial pH of all solutions was approximately 7 by using a METRIA M21 pH-meter (Labbox, Spain), as pH in drinking water should fall between the values of 6.5 and 8.5.[39] This parameter has a significant influence on the speciation of FC in a water dilution system. In acidic conditions, the predominant species is hypochlorous acid (HOCl), while in basic conditions the predominant species is the hypochlorite ion (OCl^-).[11]

The concentration of FC in the treated water was determined using the DPD (*N*,*N*-diethyl-*p*-phenylenediamine) standard method (4500-Cl G) in a PoolLab 1.0 photometer (Water-I.D., Germany), measuring in a range of 0.00 to 6.00 $mg{\cdot}L^{-1}$. For this, a DPD 1 photometer test tablet reagent (Lovibond, Germany) was added to each 10 mL water sample. DPD reacts with FC in water, changing the color from colorless to pink, and the color intensity corresponds to the concentration of available chlorine. The resulting color change was measured at a wavelength of 546 nm. The analysis was performed immediately after the samples. The FC in all of the experiments was measured in duplicate, and the average value was reported.

2.2. Electrochemical Cell and Experimental Setup. The experimental configuration used in this study is represented in Figure 1a. A volume of 60 mL of water for each experiment was dispensed through a syringe pump (KD Scientific, USA) in a flow rate range of 100−400 $mL{\cdot}h^{-1}$. The pump was coupled to the inlet Luer-lock connector (em-Technik, Germany) in the flow cell by PEEK tubing (1/4″). The treated water was collected in a 100 mL flask, from where 10 mL samples were taken for each FC analysis. Before starting a new experiment, the electrochemical reactor was rinsed with a minimum amount of 100 mL of distilled water and then washed with 60 mL of test solution. The current was supplied to the electrodes of the flow cell by a power source (RCE, Italy) capable of delivering a current of up to 10 A. The acrylic polymer plates, bolts, and current collectors of the cell are similar to the design by Martin et al.[40] The anode of the cell was connected to the positive terminal of the power supply and the cathode to the negative one through 0.5 mm planar copper current collectors. Graphite was used as the anode (active electrode surface: 616 mm^2; Eisenhüt, Germany), and stainless steel 304 was used as the cathode (active electrode surface: 616 mm^2; Gust. Alberts GmbH, Germany). Two digital multimeters (OW15E, OWON) measured the cell current and voltage continuously during the trials. The experiments were conducted at room temperature, approximately 22 °C.

As shown in Figure 1b, the main component of the flow cell is a biomimetic flow field (2 mm interelectrode gap). The flow field was designed parametrically with the software Rhinoceros and its plugin Grasshopper, according to the procedure described in our previous publications.[32,33] The model was 3D printed by stereolithography (Anycubic Photon Mono, Anycubic), using an ABS-like photopolymerizable resin (Anycubic). The residual resin was cleaned after printing with isopropyl alcohol (>99 wt %; Höfer Chemie, Germany). Finally, the flow field was subjected to a 405 nm light source for 120 s to finish the curing process. This ABS-like material has sufficient flexibility to maintain water tightness, so it avoids the use of additional sealing materials. A leakage test at the maximum flow rate was conducted on the flow cell before the experiments.

2.3. Selection of Significant Variables. The electrochlorination process is affected by many variables. The preliminary selection of the factors for the screening design was based on preliminary experiments combined with a literature review. In total, six variables ($k = 6$) were chosen, including x_1, applied current, x_2 inlet water flow rate, and x_3, x_4, x_5, and x_6, which correspond to Cl^-, SO_4^{2-}, HCO_3^-, and Ca^{2+} concentrations, respectively. These ions were identified as the most abundant in typical groundwater.[41] Different DOE approaches have been utilized to understand the impacts of several factors in water disinfection processes.[42] In this case, a DSD was used to evaluate the influence of the chosen parameters on FC production. DSD is a novel three-level DOE (coded as −1, 0 + 1) that offers advantages over standard screening designs, as it allows for the estimation of main effects as well as some second-order interactions and quadratic terms with a small number of runs, such as in refs 43,44. Table 1 indicates the nomenclature for each variable as well as the levels for the experiment in coded and uncoded units.

The selection of high- and low-level values for current and flow rate is based on preliminary experiments. For the concentration of ions, the maximum and minimum correspond to the threshold values of Secondary Drinking Water Standards[45] or the lowest typical values in

Table 1. Factors with Coded and Uncoded Levels for DSD for the Electrochlorination Process.

factor	description	unit	level		
			−1	0	+1
x_1	$[Cl^-]$	$mg{\cdot}L^{-1}$	25	137.5	250
x_2	$[SO_4^{2-}]$	$mg{\cdot}L^{-1}$	50	150	250
x_3	$[HCO_3^-]$	$mg{\cdot}L^{-1}$	50	150	250
x_4	$[Ca^{2+}]$	$mg{\cdot}L^{-1}$	10	42.5	75
x_5	flow rate	$ml{\cdot}h^{-1}$	100	250	400
x_6	current	mA	30	55	80

https://doi.org/10.1021/acssuschemeng.3c07066
ACS Sustainable Chem. Eng. 2024, 12, 3130−3141

groundwater, respectively. The total number of performed runs (N) depends on the number of variables (k) and corresponds to eq 5:

$$N = 2k + 1 \quad (5)$$

The relationship between the variables and the response may imply second-order interactions, according to eq 6

$$y_1 = b_0 + \sum b_i x_i + \sum b_{ii} x_i^2 + \sum b_{ij} x_i x_j \quad (6)$$

where y_1 indicates the measured response of active chlorine concentration, x_i and x_j are independent variables, b_0 is the offset term, b_i is the coefficient of linear parameters, b_{ij} is the coefficient for the interaction between parameters, and b_{ii} is for the interaction of quadratic terms.

The suitability of the model was evaluated through the analysis of variance (ANOVA). The R-Square value (R^2), the adjusted R-Square value (R^2adj), the predicted R-Square value (R^2pred), and the F-static for the investigated parameters were used to determine the accuracy and statistical fitness of the proposed model. The statistical significance of all model parameters was determined using a probability value of 0.05 with a 95% confidence level. The regression assumptions were verified using different diagnostic techniques, such as a graphical comparison of the predicted and experimental values, a normal probability plot of the studentized residuals, a continuous search for errors in the studentized residuals vs predicted plot, and a Box−Cox plot to determine whether power transformations were necessary.[46] Minitab 19 (Minitab, USA) software was used to evaluate the data and provide a statistical model.

2.4. Response Surface Methodology. Response surface methodology (RSM) encompasses optimization techniques aimed at adjusting the levels of factorial variables in order to achieve a desired maximum or minimum response value. The most significant parameters of the electrochlorination process obtained in the screening design described above were thus subjected to optimization. A Box−Behnken response surface design was implemented.[47] This allows to evaluate each variable over three levels with equally spaced values (coded as −1, 0, +1) but avoids the corners of space and combining central and extreme levels.[48] The Box−Behnken design enables the estimation of first- and second-order interactions with a lower number of runs than central composite designs.[49] The number of experiments required (N) is calculated according to eq 7:

$$N = 2k(k - 1) + C_0 \quad (7)$$

where k is the number of variables studied, and C_0 is the central point repetitions with response surface curves. The model for FC concentration prediction can be described as a second-order regression equation (eq. 8):

$$y' = b_0' + \sum b_i' x_i + \sum b_{ii}' x_i^2 + \sum b_{ij}' x_i x_j \quad (8)$$

Here, y' is the response value for the response surface optimization, x_i and x_j are independent variables, b_0 is the offset term, b_i is the coefficient of linear parameters, b_{ij} is the coefficient for the interaction between parameters, and b_{ii} is for the interaction of quadratic terms.[50]

Another important parameter in electrolytic processes is the energy required to obtain the compound of interest. In each of the experiments, the cell voltage supplied by the power source was measured with a multimeter equipped with a data logger. As the voltage oscillated during the experiment, average values were taken for the power consumption calculation. There are different ways to report the energy consumption in electrochemical water treatments such as current efficiency. In this study, the specific energy consumption, (SEC) (eq. 9) was considered:[26]

$$\mathrm{SEC} = \frac{iu}{Q\Delta C} \quad (9)$$

where i is the applied current (A), u is the cell voltage (V), Q is the water inlet flow rate ($L{\cdot}h^{-1}$), and ΔC is the concentration difference of FC ($mg{\cdot}L^{-1}$).

3. RESULTS

3.1. Selection of Significant Variables. Table 2 displays a matrix with the experimental conditions for the six variables in the screening design. In total, 13 runs with randomized order were carried out for measuring the concentration of FC.

Table 2. DSD experimental design matrix of six variables controlling the FC response.

	uncoded factor level						response
run	x_1 = $[Cl^-]$	x_2 = $[SO_4^{2-}]$	x_3 = $[HCO_3^-]$	x_4 = $[Ca^{2+}]$	x_5 = flow rate	x_6 = applied current	free chlorine
	$mg{\cdot}L^{-1}$	$mg{\cdot}L^{-1}$	$mg{\cdot}L^{-1}$	$mg{\cdot}L^{-1}$	$ml{\cdot}h^{-1}$	mA	$mg{\cdot}L^{-1}$
1	250.0	250	50	10.0	400	55	0.94
2	25.0	250	50	42.5	100	80	0.42
3	137.5	50	50	10.0	100	30	0.76
4	250.0	150	250	10.0	100	80	3.70
5	137.5	150	150	42.5	250	55	0.86
6	137.5	250	250	75.0	400	80	0.83
7	25.0	50	150	10.0	400	80	0.41
8	25.0	150	50	75.0	400	30	0.10
9	250.0	50	50	75.0	250	80	3.17
10	250.0	250	150	75.0	100	30	1.80
11	250.0	50	250	42.5	400	30	0.70
12	25.0	250	250	10.0	250	30	0.05
13	25.0	50	250	75.0	100	55	0.45

A normal probability plot of the FC results was established to verify whether the data fulfilled the assumption of normality. As the data was not normally distributed, the skewed data was converted into normal data using the Box−Cox transformation, depending on the power parameter (λ).[51] The optimal λ was found to be 0.20 (Supporting Information, Figure S1).

Table 3 presents the ANOVA results with a confidence level of 95%. The terms DF, Adj SS, and Adj MS indicate the total degrees of freedom, the adjusted sums of squares, and the adjusted mean squares, respectively. *F-value* is the statistic test used to determine whether any term in the model is associated with the response. The *P-value* is the probability that measures evidence against the null hypothesis. The value of the determination coefficient (R^2 = 0.9725) indicates that 97.25% of the variability in the FC response was explained by the model. The value of the adjusted determination

Table 3. ANOVA results for the FC response in the DSD study.[a]

source	DF	adj SS	adj MS	*F*-value	*P*-value
model	6	0.579014	0.096502	35.31	0.000
linear	6	0.579014	0.096502	35.31	0.000
x_1 = $[Cl^-]$	1	0.391125	0.391125	143.10	0.000
x_2 = $[SO_4^{2-}]$	1	0.013994	0.013994	5.12	0.064
x_3 = $[HCO_3^-]$	1	0.000503	0.000503	0.18	0.683
x_4 = $[Ca^{2+}]$	1	0.004826	0.004826	1.77	0.232
x_5 = flow rate	1	0.055930	0.055930	20.46	0.004
x_6 = current	1	0.112636	0.112636	41.21	0.001
error	6	0.016400	0.002733		
total	12	0.595414			

[a] R^2 = 97.03%; R^2-adj = 91.69%; R^2-pred = 55.20%.

https://doi.org/10.1021/acssuschemeng.3c07066
ACS Sustainable Chem. Eng. 2024, 12, 3130−3141

coefficient (R^2_{adj} = 0.9449) was close to the determination coefficient, demonstrating high significance in the model. Based on the regression analysis, the equation was adjusted to the empirical data, as shown in eq 10:

$$FC^{0.20} = 0.6236 + 1.758\cdot10^{-3}x_1 - 3.74\cdot10^{-4}x_2 - 7.1\cdot10^{-5}x_3 + 6.76\cdot10^{-4}x_4 - 4.99\cdot10^{-4}x_5 + 4.25\cdot10^{-3}x_6 \quad (10)$$

The most significant variables were the initial concentration of chlorides (p = 0.000), the applied current (p = 0.001), and the water flow rate (p = 0.004) because the p-values are less than the significance level of 0.05. A graphical representation of these results is also shown in a Pareto plot (Figure 2a). Runs 4

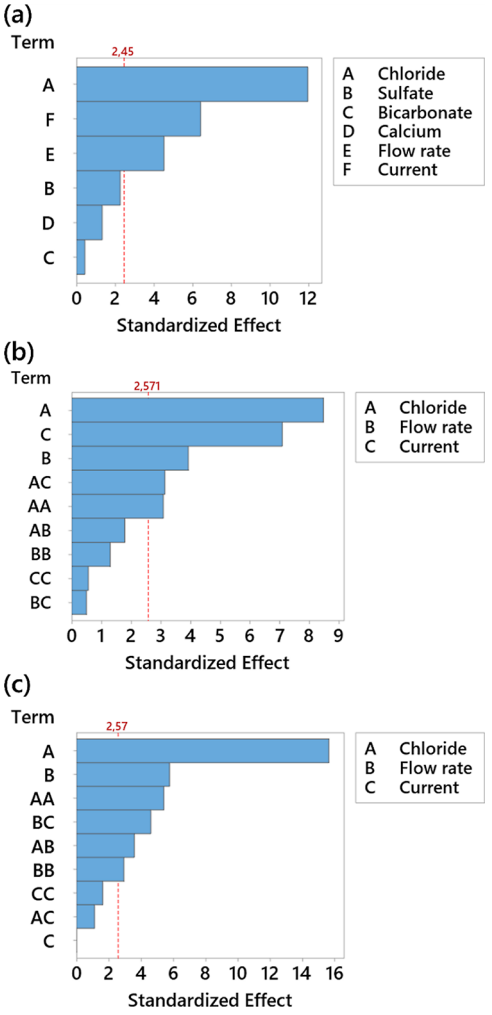

Figure 2. Pareto plot standardized effects. (a) FC in the DSD, (b) FC in the Box–Behnken design, and (c) SEC responses in the Box–Behnken design.

and 9 resulted in the maximum chlorine concentration corresponding to the high chloride concentrations of 250 mg·L^{-1} and high applied currents of 80 mA. In the observed experimental conditions, the roles of variables such as sulfate, bicarbonate, and calcium concentrations, as well as flow rates, were comparatively secondary in influencing the system's performance relative to the more pronounced effects of chloride ion concentration and applied current. The rate of the chlorine synthesis step is determined by the availability of chloride ions at the anode surface, hence higher chloride concentrations improve chlorine production.[25,52,53] Moreover, the conductivity of the solution is increased at a higher chloride concentration, decreasing the ohmic drop in the solution. Increasing the applied current also increases the amount of product during electrochlorination. Higher applied current enhances the electron-transfer rate, too, increasing chorine production below the limiting current region. Finally, reducing the water flow rate increases the residence time and the opportunities for the chloride ions to convert at the anode. At higher flow rates, the residence time of water in the electrochemical cell is reduced. This shorter contact time between the water and the electrodes may lead to insufficient interaction for complete chlorine generation. This effect was also reported in previous studies.[54,55] These trends are represented in a main effects plot (Supporting Information, Figure S2). The results of these experiments are in agreement with previous studies.[56,57] These variables were selected for further optimization study.

Even though the concentration of nonelectroactive ions is not significant in this model, their presence in water cannot be avoided and could decrease the total chlorine generation at the anode. These ions increase the conductivity of the solution, but it has been reported that nonelectroactive ions compete with the transfer of chloride ions inside the electrical double layer (EDL).[58] Polyvalent ions, such as sulfates, occupy a position in the EDL prior to monovalent ions, such as chlorides, as they have faster migration rates, obstructing access to chloride ions. In previous studies, a molar ratio concentration of nonelectroactive ion/chloride ion equal to 0.25 showed 75% inhibition over active chlorine production.[59] In this work, any possible inhibition effects by the non-electroactive ions are implicit in the regression for the chosen typical water source compositions.

Previous studies reported that electro-oxidation occurring at the anode can result in the production of chlorine radicals ($Cl^{\bullet}$) and dichloride radicals ($Cl_2^{\bullet-}$) through the interaction of sulfate radicals with chloride ions (Cl^-).[60] The presence of other species such as persulfate ($S_2O_8^{2-}$) or radicals like sulfate ($SO_4^{\bullet-}$), and carbonate ($CO_3^{\bullet-}$), especially when their respective anions are present,[61,62] has also been reported.

On the other hand, the presence of magnesium and calcium ions at low concentrations can eventually generate a precipitate at the cathode. It has been reported that $Ca(OH)_2$ deposits inhibit, in particular, hypochlorite production.[63] Naturally, cathodic precipitates can be removed physically or chemically by cleaning the cell when they become detrimental.

3.2. RSM. Once the most significant variables were selected in the preliminary screening, a Box–Behnken design was implemented to determine the optimal operation regions in terms of FC generation and energy consumption. Table 4 shows the Box–Behnken experimental design (15 runs) with the three most significant parameters (chloride, flow rate, and applied current) from the screening design. The concentrations of SO_4^{2-}, HCO_3^-, and Ca^{2+} were constant, with the following values: 150, 150, and 42.5 mg·L^{-1}, respectively. These values correspond to the average concentrations tested in the preliminary screening design.

According to the normal probability plot, the FC response was normally distributed and the variances were homogeneous. Thus, a data transformation was not required. On the contrary, the SEC response was converted using the Box–Cox power

https://doi.org/10.1021/acssuschemeng.3c07066
ACS Sustainable Chem. Eng. 2024, 12, 3130−3141

Table 4. Experimental matrix of Box–Behnken design, including FC production and SEC.

run	x_1 = [Cl^-]	x_5 = flow rate	x_6 = current	FC	SEC
	$mg·L^{-1}$	$ml·h^{-1}$	mA	$mg·L^{-1}$	$Wh·mg\ FC^{-1}$
1	25.0	400	55	0.120	9.84
2	137.5	250	55	1.500	0.90
3	137.5	250	55	1.765	0.77
4	250.0	100	55	3.100	1.18
5	25.0	250	80	0.350	10.28
6	137.5	100	30	1.440	1.23
7	25.0	100	55	0.395	14.30
8	137.5	400	30	0.315	1.41
9	250.0	250	30	1.000	0.65
10	25.0	250	30	0.210	3.99
11	137.5	100	80	3.400	2.51
12	250.0	250	80	3.200	0.67
13	137.5	250	55	1.600	0.77
14	137.5	400	80	2.600	0.58
15	250.0	400	55	1.650	0.42

parameter equal to −0.5 (Supporting Information, Figure S3). Table 5 represents the ANOVA for the two responses in the Box–Behnken design. For the FC response, the three independent variables, i.e., the quadratic term of chloride concentration and the interaction between chlorides and applied current, were statistically significant ($p < 0.05$). These results are also represented in a Pareto plot (Figure 2b). As the p-value > α, the lack-of-fit is not statistically significant. The R^2 value indicates that the empirical model can be applied to foresee the FC values with 97.03% confidence. The adjusted R^2 was 0.9169. In the case of the SEC, the linear terms of chloride concentration and flow rate were statistically significant, as well as its quadratic terms and the interactions between chlorides and flow rate and the flow rate and current (Figure 2c). The lack-of-fit was also not statistically significant. The R^2 value was 98.59%, and the R^2-adj value was 96.06%. Parity plots for both FC and SEC responses of the observed against predicted responses are shown in Figure 3. The regression equations correspond to eqs. 11 and 12:

$$FC = 0.74 + 0.014\,x_1 - 6.8\cdot10^{-3}\,x_5 - 0.0145\,x_6 - 4.2\cdot10^{-5}\,x_1x_1 + 1\cdot10^{-5}\,x_5x_5 + 1.53\cdot10^{-4}\,x_6x_6 - 1.7\cdot10^{-5}\,x_1x_5 + 1.8\cdot10^{-4}\,x_1x_6 + 2.2\cdot10^{-5}\,x_5x_6 \quad (11)$$

$$-SEC^{-0.5} = -0.384 - 5.83\cdot10^{-3}\,x_1 + 6\cdot10^{-5}\,x_5 + 2.6\cdot10^{-3}\,x_6 + 1.8\cdot10^{-5}\,x_1x_1 + 5\cdot10^{-6}\,x_5x_5 + 1.08\cdot10^{-4}\,x_6x_6 - 8\cdot10^{-6}\,x_1x_5 - 1.6\cdot10^{-5}\,x_1x_6 - 4.9\cdot10^{-5}\,x_5x_6 \quad (12)$$

The relationship between the independent variables and the FC response, holding the chloride concentration, is represented by the three-dimensional plots and two-dimensional contour plots (Figure 4). The graphs indicate that the chlorine generation increases gradually with increasing the chloride concentration and applied current while decreasing when increasing the flow rate, as predicted in the screening design [also shown in Supporting Information, Figures S4(a) and S5(a)]. The WHO chlorination guidelines indicate FC residuals of at least 0.5 $mg·L^{-1}$ throughout the distribution system and at least 0.2 $mg·L^{-1}$ at the point of delivery for piped infrastructure. In the case of residential POU water treatment, the residual should be larger than 0.2 mg/L but not greater than 2.0 $mg·L^{-1}$,[64] normally not exceeding 1 $mg·L^{-1}$.[65] Higher chlorine doses affect water taste and odor and can make people averse to drinking chlorinated water.[66] According to studies on the taste of chlorinated water, users will refuse to drink chlorinated water above a particular concentration threshold due to the unpleasant taste.[67] Then, the operation conditions (applied current and flow rate) for the electrochlorination cell should be established for chlorine generation higher than 0.2 $mg·L^{-1}$ but below 2.0 $mg·L^{-1}$ according to Figure 4 for drinking water.

Table 5. ANOVA results for the FC and SEC responses in the Box–Behnken design.[a]

	FC					SEC				
source	DF	Adj SS	Adj MS	F-value	P-value	DF	Adj SS	Adj MS	F-value	P-value
model	9	176.025	195.583	18.15	0.003	9	223.748	0.24861	38.90	0.000
linear	3	148.375	494.585	45.91	0.000	3	177.657	0.59219	92.67	0.000
x_1 = [Cl^-]	1	77.520	775.195	71.95	0.000	1	156.352	156.352	244.67	0.000
x_5 = flow rate	1	16.653	166.531	15.46	0.011	1	0.21305	0.21305	33.34	0.002
x_6 = current	1	54.203	542.028	50.31	0.001	1	0.00000	0.00000	0.00	0.996
square	3	13.325	0.44416	4.12	0.081	3	0.23499	0.07833	12.26	0.010
x_1^2	1	10.258	102.579	9.52	0.027	1	0.18715	0.18715	29.29	0.003
x_5^2	1	0.1814	0.18143	1.68	0.251	1	0.05538	0.05538	8.67	0.032
x_6^2	1	0.0336	0.03362	0.31	0.601	1	0.01679	0.01679	2.63	0.166
2-way interaction	3	14.325	0.47749	4.43	0.071	3	0.22592	0.07531	11.78	0.011
x_1*x_5	1	0.3452	0.34516	3.20	0.133	1	0.08226	0.08226	12.87	0.016
x_1*x_6	1	10.609	106.090	9.85	0.026	1	0.00795	0.00795	1.24	0.315
x_5*x_6	1	0.0264	0.02641	0.25	0.642	1	0.13571	0.13571	21.24	0.006
error	5	0.5387	0.10774			5	0.03195	0.00639		
lack-of-fit	3	0.5029	0.16763	9.36	0.098	3	0.02718	0.00906	3.79	0.216
pure error	2	0.0358	0.01791			2	0.00477	0.00239		
total	14	181.412				14	226.944			

[a] R^2 = 97.03%; R^2-adj = 91.69%; R^2-pred = 55.20% R^2 = 98.59%; R^2-adj = 96,06%; R^2-pred = 80,37%.

https://doi.org/10.1021/acssuschemeng.3c07066
ACS Sustainable Chem. Eng. 2024, 12, 3130−3141

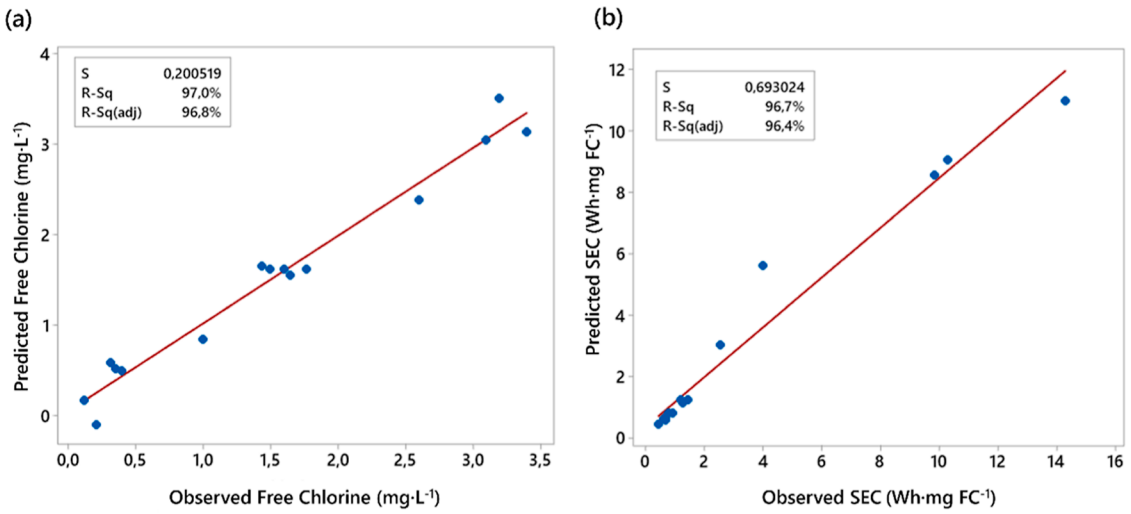

Figure 3. Parity plot in the Box–Behnken design. (a) FC and (b) SEC responses.

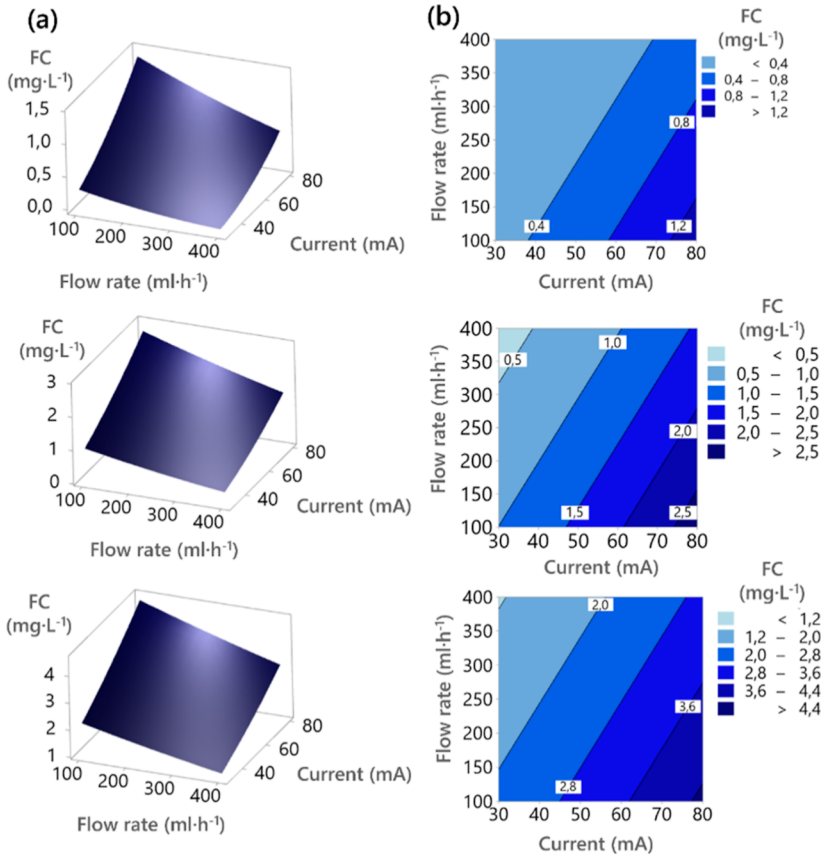

Figure 4. FC generation for different initial chloride concentrations; from top to bottom: $[Cl^-]$ = 25, 137.5 and 250 mg·L^{-1}, respectively. (a) 3D surface plot and (b) 2D contour plots.

Both applied current and flow rate also play an important role in the generation of electrochlorination byproducts, such as chlorate (ClO_3^-) and perchlorate (ClO_4^-). Chloride ions can suffer oxidation to produce higher oxychlorine species, as per eq 13:[68]

$$Cl^- \rightarrow OCl^- \rightarrow ClO_2^- \rightarrow ClO_3^- \rightarrow ClO_4^- \quad (13)$$

According to previous studies, the concentration of both species increases by increasing the electrolysis time and for high overpotentials. Indeed, these factors increase the possibility of the active chlorine species to be oxidized.[69] Studies suggest that the decomposition of hypochlorite follows a second-order reaction, so that the formation of chlorate and perchlorate are increased by higher concentrations of hypochlorite.[70,71] It has also been proposed that the chloride concentration in the solution has an effect on chlorate formation.[72] In this study, the maximum applied current density was 129.4 versus 1500 A·m^{-2}, one order of magnitude lower than the currents reported in the first mentioned study.[69] The longest electrolysis time in this single pass flow cell is 44.3

https://doi.org/10.1021/acssuschemeng.3c07066
ACS Sustainable Chem. Eng. 2024, 12, 3130–3141

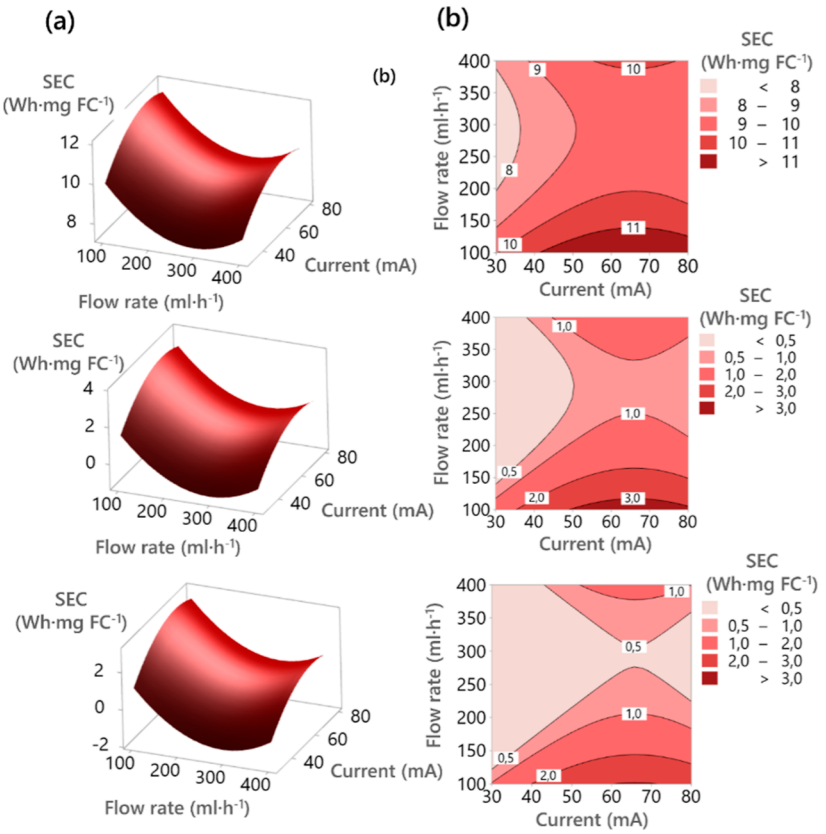

Figure 5. SEC for different initial chloride concentrations, from top to bottom: $[Cl^-]$ = 25, 137.5, and 250 mg·L^{-1}, respectively. (a) 3D surface plot and (b) 2D contour plots.

s, corresponding to the lower flow rate, which is typically lower than the electrolysis time for a batch reactor or flow reactor in recirculation mode. Moreover, both the initial chloride concentration and FC species were kept low during the experiments. For these reasons, the formation of significant amounts of chlorate and perchlorate is not expected with the proposed electrochemical reactor configuration.

Figure 5 presents the 3D and 2D contour plots for the SEC values for each initial chloride concentration, considering the variations in the applied current and flow rate. The interaction between flow rate and applied current was indicated by a saddle point. This corresponds to the inflection point between a relative maximum and a relative minimum.[50] The main effects and interaction plots are also represented in Supporting Information, Figures S4(b) and S5(b). The SEC ranged from 0.42 to 14.30 Wh·mg Cl_2^{-1} generated, depending mainly on the chloride concentration in water.[25] Assuming that the desired chlorine concentration in drinking water was 0.5 mg·L^{-1}, the energy consumption per cubic meter treated would be 0.21 to 7.15 kWh·m^{-3}. When the ionic conductivity diminishes, the corresponding solution resistance of the system increases, resulting in an increase in the voltage when it is operated at a constant electrical current. This decrease in current consequently leads to reduced production of oxidants.[73]

The reported energy consumption for electrochlorination varies considerably depending on the operating conditions and type of electrochlorination system. Studies on electrochlorination have documented a broad range from 0.01 to 100 kWh·m^{-3}, for achieving 2 mg·L^{-1} of chlorine concentration.[74] For instance, the Zappi cell (with platinum-clad niobium mesh anodes) in the presence of 0.01 M NaCl electrolyte consumed approximately 6.3 kWh·m^{-3}.[75] An investigation reported lower energy consumptions of 0.0145 to 0.0159 kWh·g^{-1} of FC from chloride concentrations between 710 and 1.775 mg·L^{-1}. The authors used an undivided filter-press lab-scale electrolyzer equipped with a Ti|Ti−Ru−Ir-oxides anode and a stainless-steel cathode.[53] In another reactor configuration, including cylindrical graphite anodes and stainless steel cathodes, with a chloride concentration of 50 mg·L^{-1}, the reported energy consumption was 0.083 kWh·m^{-3} for an FC generation of 2 mg·L^{-1}.[76] The differences in energy consumption between these studies and the one reported in this study could be attributed to the differences in the anode material in the first case and the residence times employed. On the one hand, the metal oxides anodes are known to have better chlorine-generation efficiency than graphite.[77,78] On the other hand, while our cell has a continuous operation with residence times between 12 and 48 s, the above-mentioned reactors operated with recirculation with a residence time of 240 min and in batch mode with a residence time of 50 min. This variation in residence time can considerably influence chloride conversion.[25]

The higher energy demands in electrochlorination could limit its use for treating large volumes of water but remain practical for smaller applications processing only a few liters daily.[26] An economic evaluation of these smaller systems in various rural locations revealed that, in comparison to the upfront investment and other maintenance expenses, the energy costs were relatively insignificant.[79]

In order to optimize the system, the effects of operation conditions on the two responses (FC generation and SEC)

https://doi.org/10.1021/acssuschemeng.3c07066
ACS Sustainable Chem. Eng. 2024, 12, 3130−3141

were studied by a composite desirability analysis. In this case, the optimization intends to minimize the SEC to produce a constant value of FC of 0.5 mg·L^{-1}. The desirability function converts an estimated response into a scale-free value called desirability. The values of desirability functions are between 0 and 1, where 0 corresponds to an undesirable response and 1 to the optimal performance of the independent factors.[80] Table 6 shows the operation conditions and response values for composite desirability analysis. The composite desirability for each chloride composition is close to 1, indicating that the operation parameters reach favorable results for the two responses. Then, the optimal flow rates are 371, 388, and 400 mL·h^{-1} and the applied current 75.8, 30.0, and 35.5 mA for chloride content of 25, 137.5, and 250 mg·L^{-1}, respectively.

Table 6. Composite Desirability Analysis Results for FC Generation at Different Initial Chloride Concentrations

x_1 = [Cl$^-$]	x_5 = flow rate	x_6 = current	free chlorine	SEC	composite desirability
mg·L^{-1}	ml·h^{-1}	mA	mg·L^{-1}	Wh·mg FC^{-1}	
25	371	75.8	0.50	5.67	0.80
137.5	388	30.0	0.58	1.17	0.96
250	400	35.5	0.50	0.59	0.99

It is important to mention that no fouling by formation of calcium or magnesium hydroxide scales was observed at the electrodes during these tests. However, hard water (with high levels of such ions) can eventually affect electrochlorination performance due to the formation of deposits on the electrode surfaces, hindering chlorine production.[81] Such cathode fouling problems are common and are typically addressed through the use of cleaning agents or mechanical methods, in addition to higher levels of mixing and turbulence in the flow cell.[81] Alternatively, the polarity of two electrodes of equal composition can be switched over time, as shown with DSA or Ebonex electrodes.[82] These types of electrodes would increase the cost of the electrochlorination system but could be considered for further applications outside of low-cost settings.

On the other hand, the concept of sustainability implies technical, environmental, technical, and social aspects. The electrochemical flow cell developed here contributes to sustainability across these dimensions. Environmentally, the cell design for efficient chlorine generation from low chloride concentrations minimizes the additional use of substances and supports renewable energy integration. Technically, the reactor is applicable in varied water compositions, demonstrating reliability in chlorine generation, scalable capacity, low complexity, reduced waste generation, and low land requirements. Socially, it aims to facilitate water disinfection in low-resource, decentralized settings, addressing public health needs. Economically, the low-cost, minimal material requirement, along with the SEC optimization, contributes to its financial feasibility and resource efficiency, aiming for a sustainable application in different contexts.

4. CONCLUSIONS

A novel electrochemical flow cell with a 3D-printed biomimetic flow field has been proposed for electrochlorination in decentralized water disinfection. A compact electrochemical reactor is enabled by the intricate channel, which favors long residence−time reactions in a reduced volume. The main advantage of this reactor is its ability to operate without the need for water recirculation or sodium chloride dosing, thanks to its combination of high mass transfer and simple design. This feature simplifies the electrochlorination process and reduces the need for additional materials and logistics commonly associated with traditional systems. In contrast, traditional electrochlorinators typically operate at high chloride concentrations, which can indeed increase the current efficiency of the system. An experimental design permitted us to establish the main factors affecting FC generation, including the concentration of several ions in water, flow rate, and applied current. Screening tests then revealed the predominant influence of chloride concentration, flow rate, and applied current. The results demonstrated the possibility of generating a suitable amount of FC for disinfection from chloride ions naturally present in source water, even at a low concentration of 25 mg·L^{-1}. The optimization of operation parameters was carried out with a Box−Behnken design, considering the SEC to generate chlorine in each experiment. The composite desirability analysis suggested optimal flow rates between 371 and 400 mL·h^{-1} and applied current 75.8−35.5 mA for chloride ion content of 25 to 250 mg·L^{-1}. These results open up the possibility of scaling-up this electrochemical cell design to treat a higher water flow rate in a single-pass and demonstrate that the cell could be used for other electrochemical processes after a selection of adequate electrode materials and operation conditions.

■ ASSOCIATED CONTENT

Supporting Information

The Supporting Information is available free of charge at https://pubs.acs.org/doi/10.1021/acssuschemeng.3c07066.

Photograph of the experimental arrangement used in this work, Box−Cox transformation plots and main effects plots for the DSD and Box−Behnken design, and interaction plots for the Box−Behnken design (PDF)

■ AUTHOR INFORMATION

Corresponding Author

Inmaculada García-López − *Research Group Catalysis & Separation Processes (CYPS), Department of Chemical and Materials Engineering, Universidad Complutense de Madrid, Madrid 28040, Spain;* orcid.org/0000-0003-4285-3442; Email: inmgarci@ucm.es

Authors

Luis Fernando Arenas − *Research Group Applied Electrochemistry & Catalysis (ELCAT), University of Antwerp, Wilrijk 2610, Belgium*

Jonas Hereijgers − *Research Group Applied Electrochemistry & Catalysis (ELCAT), University of Antwerp, Wilrijk 2610, Belgium*

Vicente Ismael Águeda − *Research Group Catalysis & Separation Processes (CYPS), Department of Chemical and Materials Engineering, Universidad Complutense de Madrid, Madrid 28040, Spain*

Amalio Garrido-Escudero − *Research Group Catalysis & Separation Processes (CYPS), Department of Chemical and Materials Engineering, Universidad Complutense de Madrid, Madrid 28040, Spain*

Complete contact information is available at: https://pubs.acs.org/10.1021/acssuschemeng.3c07066

Notes

The authors declare no competing financial interest.

REFERENCES

(1) World Health Organization. *Progress on Household Drinking Water, Sanitation and Hygiene 2000−2017: Special Focus on Inequalities*; World Health Organization, 2019.

(2) Hossain, M. A.; Sengupta, M. K.; Ahamed, S.; Rahman, M. M.; Mondal, D.; Lodh, D.; Das, B.; Nayak, B.; Roy, B. K.; Mukherjee, A.; Chakraborti, D. Ineffectiveness and Poor Reliability of Arsenic Removal Plants in West Bengal, India. *Environ. Sci. Technol.* **2005**, *39* (11), 4300−4306.

(3) Drinking-water. https://www.who.int/news-room/fact-sheets/detail/drinking-water (accessed Oct 25, 2022).

(4) Kumar, M. D.; Tortajada, C. Health Impacts of Water Pollution and Contamination Assessing Wastewater Management in India Kumar, M. D., Tortajada, C., Eds.; SpringerBriefs in Water Science and Technology; Springer: Singapore, 2020, pp 23−30..

(5) Pooi, C. K.; Ng, H. Y. Review of Low-Cost Point-of-Use Water Treatment Systems for Developing Communities. *Npj Clean Water* **2018**, *1* (1), 11−18.

(6) Sobsey, M. D.; Stauber, C. E.; Casanova, L. M.; Brown, J. M.; Elliott, M. A. Point of Use Household Drinking Water Filtration: A Practical, Effective Solution for Providing Sustained Access to Safe Drinking Water in the Developing World. *Environ. Sci. Technol.* **2008**, *42* (12), 4261−4267.

(7) Lindmark, M.; Cherukumilli, K.; Crider, Y. S.; Marcenac, P.; Lozier, M.; Voth-Gaeddert, L.; Lantagne, D. S.; Mihelcic, J. R.; Zhang, Q. M.; Just, C.; Pickering, A. J. Passive In-Line Chlorination for Drinking Water Disinfection: A Critical Review. *Environ. Sci. Technol.* **2022**, *56* (13), 9164−9181.

(8) Dandie, C. E.; Ogunniyi, A. D.; Ferro, S.; Hall, B.; Drigo, B.; Chow, C. W. K.; Venter, H.; Myers, B.; Deo, P.; Donner, E.; Lombi, E. Disinfection Options for Irrigation Water: Reducing the Risk of Fresh Produce Contamination with Human Pathogens. *Crit. Rev. Environ. Sci. Technol.* **2020**, *50* (20), 2144−2174.

(9) Mintz, E.; Bartram, J.; Lochery, P.; Wegelin, M. Not Just a Drop in the Bucket: Expanding Access to Point-of-Use Water Treatment Systems. *Am. J. Public Health* **2001**, *91* (10), 1565−1570.

(10) Nielsen, A. M.; Garcia, L. A. T.; Silva, K. J. S.; Sabogal-Paz, L. P.; Hincapié, M.; Montoya, L. J.; Galeano, L.; Galdos-Balzategui, A.; Reygadas, F.; Herrera, C.; Golden, S.; Byrne, J. A.; Fernández-Ibáñez, P. Chlorination for Low-Cost Household Water Disinfection - A Critical Review and Status in Three Latin American Countries. *Int. J. Hyg. Environ. Health* **2022**, *244*, 114004.

(11) Kraft, A.; Stadelmann, M.; Blaschke, M.; Kreysig, D.; Sandt, B.; Schröder, F.; Rennau, J. Electrochemical Water Disinfection Part I: Hypochlorite Production from Very Dilute Chloride Solutions. *J. Appl. Electrochem.* **1999**, *29* (7), 859−866.

(12) Rusling, J. F. Environmental Electrochemistry: Fundamentals and Applications in Pollution Abatement By Krishnan Rajeshwar (University of Texas at Arlington) and Jorge G. Ibanez (Universidad IberoAmericana). Academic Press: San Diego. 1996. $95.00. xvi + 776 pp. ISBN 0-12-576260-7. *J. Am. Chem. Soc.* **1998**, *120* (45), 11837.

(13) Abdul-Wahab, S. A.; Al-Weshahi, M. A. Brine Management: Substituting Chlorine with On-Site Produced Sodium Hypochlorite for Environmentally Improved Desalination Processes. *Water Resour. Manage.* **2009**, *23* (12), 2437−2454.

(14) Gusmão, I. C. C. P.; Moraes, P. B.; Bidoia, E. D. Studies on the Electrochemical Disinfection of Water Containing Escherichia Coli Using a Dimensionally Stable Anode. *Braz. Arch. Biol. Technol.* **2010**, *53*, 1235−1244.

(15) Atrashkevich, A.; Alum, A.; Stirling, R.; Abbaszadegan, M.; Garcia-Segura, S. Approaching Easy Water Disinfection for All: Can in Situ Electrochlorination Outperform Conventional Chlorination under Realistic Conditions? *Water Res.* **2024**, *250*, 121014.

(16) Chinello, E.; H Hashemi, S. M.; Psaltis, D.; Moser, C. Editors' Choice-Solar-Electrochemical Platforms for Sodium Hypochlorite Generation in Developing Countries. *J. Electrochem. Soc.* **2019**, *166* (12), E336−E346.

(17) Mook, W. T.; Aroua, M. K.; Issabayeva, G. Prospective Applications of Renewable Energy Based Electrochemical Systems in Wastewater Treatment: A Review. *Renewable Sustainable Energy Rev.* **2014**, *38*, 36−46.

(18) Gray, N. F. Chapter Thirty-One - Free and Combined Chlorine. In *Microbiology of Waterborne Diseases*, 2nd ed.; Percival, S. L.; Yates, M. V.; Williams, D. W.; Chalmers, R. M.; Gray, N. F., Eds.; Academic Press: London, 2014; pp 571-590. .

(19) Palmas, S.; Mascia, M.; Vacca, A.; Mais, L.; Corgiolu, S.; Petrucci, E. Chapter 16 - Practical Aspects on Electrochemical Disinfection of Urban and Domestic Wastewater. In *Electrochemical Water and Wastewater Treatment*; Martínez-Huitle, C. A., Rodrigo, M. A., Scialdone, O., Eds.; Butterworth-Heinemann, 2018, pp 421−447..

(20) Wilson, R. E.; Stoianov, I.; O'Hare, D. Continuous Chlorine Detection in Drinking Water and a Review of New Detection Methods. *Johnson Matthey Technol. Rev.* **2019**, *63* (2), 103−118.

(21) Lucio, A. J.; Macpherson, J. V. Combined Voltammetric Measurement of PH and Free Chlorine Speciation Using a Micro-Spot Sp2 Bonded Carbon-Boron Doped Diamond Electrode. *Anal. Chem.* **2020**, *92* (24), 16072−16078.

(22) Martínez-Huitle, C. A.; Rodrigo, M. A.; Sirés, I.; Scialdone, O. Single and Coupled Electrochemical Processes and Reactors for the Abatement of Organic Water Pollutants: A Critical Review. *Chem. Rev.* **2015**, *115* (24), 13362−13407.

(23) Sirés, I.; Brillas, E.; Oturan, M. A.; Rodrigo, M. A.; Panizza, M. Electrochemical Advanced Oxidation Processes: Today and Tomorrow. A Review. *Environ. Sci. Pollut. Res.* **2014**, *21* (14), 8336−8367.

(24) Bhattacharya, M.; Bandyopadhyay, K.; Gupta, A. Design of a Cost-Effective Electrochlorination System for Point-of-Use Water Treatment. *Environ. Eng. Res.* **2020**, *26* (5), 200437.

(25) Choi, J.; Shim, S.; Yoon, J. Design and Operating Parameters Affecting an Electrochlorination System. *J. Ind. Eng. Chem.* **2013**, *19* (1), 215−219.

(26) Ocasio, D.; Sedlak, D. L. Membrane-Assisted Electrochlorination for Zero-Chemical-Input Point-of-Use Drinking Water Disinfection. *ACS EST Eng.* **2022**, *2* (10), 1933−1941.

(27) Palmas, S.; Polcaro, A. M.; Vacca, A.; Mascia, M.; Ferrara, F. Influence of the Operating Conditions on the Electrochemical Disinfection Process of Natural Waters at BDD Electrodes. *J. Appl. Electrochem.* **2007**, *37* (11), 1357−1365.

(28) Noël, T.; Cao, Y.; Laudadio, G. The Fundamentals Behind the Use of Flow Reactors in Electrochemistry. *Acc. Chem. Res.* **2019**, *52* (10), 2858−2869.

(29) Leitz, F. B.; Marinčić, L. Enhanced Mass Transfer in Electrochemical Cells Using Turbulence Promoters. *J. Appl. Electrochem.* **1977**, *7* (6), 473−484.

(30) Differential Growth - The Different Design. https://thedifferentdesign.com/digitaldownloads/differential-growth/ (accessed Nov 23, 2022).

(31) Bachman, D. Procedural Organic Modeling ACM SIGGRAPH 2019 Educators Forum. In *SIGGRAPH '19; Association for Computing Machinery*; ACM: New York, NY, USA, 2019, pp 1−59..

(32) García-López, I.; Arenas, L. F.; Turek, T.; Águeda, V. I.; Garrido-Escudero, A. Mass Transfer Enhancement in Electrochemical Flow Cells through 3D-Printed Biomimetic Channels. *React. Chem. Eng.* **2023**, *8* (7), 1776−1784.

(33) García-López, I.; Águeda, V. I.; Garrido-Escudero, A. Hydrodynamic Behavior of a Novel 3D-Printed Nature-Inspired Microreactor with a High Length-to-Surface Ratio. *Chem. Eng. J. Adv.* **2023**, *13*, 100438.

(34) Ray, C.; Jain, R. Chapter 4 - Disinfection Systems. In *Low Cost Emergency Water Purification Technologies*; Ray, C., Jain, R., Eds.; Butterworth-Heinemann: Oxford, 2014, pp 55−86..

(35) Backer, H. 5 - Water Disinfection for International Travelers. In *Travel Medicine* 4th ed.; Keystone, J. S.; Kozarsky, P. E.; Connor, B. A.; Nothdurft, H. D.; Mendelson, M.; Leder, K., Eds.; Elsevier: London, 2019; pp 31-41. .

https://doi.org/10.1021/acssuschemeng.3c07066
ACS Sustainable Chem. Eng. 2024, 12, 3130−3141

(36) Antony, J. 2 - Fundamentals of Design of Experiments Design of Experiments for Engineers and Scientists 2nd ed; Antony, J., Ed.; Elsevier: Oxford, 2014; pp 7-17. .
(37) Jones, B.; Nachtsheim, C. J. Effective Design-Based Model Selection for Definitive Screening Designs. *Technometrics* **2017**, *59* (3), 319−329.
(38) Ferreira, S. L. C.; Bruns, R. E.; Ferreira, H. S.; Matos, G. D.; David, J. M.; Brandão, G.; da Silva, E. G. P.; Portugal, L. A.; dos Reis, P. S.; Souza, A. S.; dos Santos, W. N. L. Box-Behnken Design: An Alternative for the Optimization of Analytical Methods. *Anal. Chim. Acta* **2007**, *597* (2), 179−186.
(39) World Health Organization. *Guidelines for Drinking-Water Quality: Second Addendum. Vol. 1, Recommendations*; World Health Organization, 2008.
(40) Martin, J.; Schafner, K.; Turek, T. Preparation of Electrolyte for Vanadium Redox-Flow Batteries Based on Vanadium Pentoxide. *Energy Technol.* **2020**, *8* (9), 2000522.
(41) Huang, T.; Ma, B. The Origin of Major Ions of Groundwater in a Loess Aquifer. *Water* **2019**, *11* (12), 2464.
(42) Khawaga, R.; Abouleish, M.; Abdel Jabbar, N.; Al-Asheh, S. Chlorination Breakpoint with Nitrite in Wastewater Treatment: A Full Factorial Design Experiments. *J. Environ. Chem. Eng.* **2021**, *9* (1), 104903.
(43) Fidaleo, M.; Lavecchia, R.; Petrucci, E.; Zuorro, A. Application of a Novel Definitive Screening Design to Decolorization of an Azo Dye on Boron-Doped Diamond Electrodes. *Int. J. Environ. Sci. Technol.* **2016**, *13* (3), 835−842.
(44) Jones, B.; Nachtsheim, C. J. A Class of Three-Level Designs for Definitive Screening in the Presence of Second-Order Effects. *J. Qual. Technol.* **2011**, *43* (1), 1−15.
(45) Dietrich, A. M.; Burlingame, G. A. Critical Review and Rethinking of USEPA Secondary Standards for Maintaining Organoleptic Quality of Drinking Water. *Environ. Sci. Technol.* **2015**, *49* (2), 708−720.
(46) Shukla, B. K.; Rawat, S.; Gautam, M. K.; Bhandari, H.; Garg, S.; Singh, J. Photocatalytic Degradation of Orange G Dye by Using Bismuth Molybdate: Photocatalysis Optimization and Modeling via Definitive Screening Designs. *Molecules* **2022**, *27* (7), 2309.
(47) Peng, X.; Yang, G.; Shi, Y.; Zhou, Y.; Zhang, M.; Li, S. Box-Behnken Design Based Statistical Modeling for the Extraction and Physicochemical Properties of Pectin from Sunflower Heads and the Comparison with Commercial Low-Methoxyl Pectin. *Sci. Rep.* **2020**, *10* (1), 3595.
(48) Rakić, T.; Kasagić-Vujanović, I.; Jovanović, M.; Jančić-Stojanović, B.; Ivanović, D. Comparison of Full Factorial Design, Central Composite Design, and Box-Behnken Design in Chromatographic Method Development for the Determination of Fluconazole and Its Impurities. *Anal. Lett.* **2014**, *47* (8), 1334−1347.
(49) Hanrahan, G.; Lu, K. Application of Factorial and Response Surface Methodology in Modern Experimental Design and Optimization. *Crit. Rev. Anal. Chem.* **2006**, *36* (3−4), 141−151.
(50) Bezerra, M. A.; Santelli, R. E.; Oliveira, E. P.; Villar, L. S.; Escaleira, L. A. Response Surface Methodology (RSM) as a Tool for Optimization in Analytical Chemistry. *Talanta* **2008**, *76* (5), 965−977.
(51) Box, G. E.; Cox, D. R. An Analysis of Transformations. *J. R. Stat. Soc. Ser. B, Methodol.* **1964**, *26* (2), 211−243.
(52) Shinde, S. R.; Apte, S. Correlation Analysis of the Experimental Data for In-Situ Chlorine Generation in Electrochlorination Process. *J. Environ. Eng.* **2023**, *149* (4), 04023004.
(53) Rodríguez, J. F.; Nava, J. L. Active Chlorine Electrosynthesis from Dilute Chloride Solutions in a Flow Cell Equipped with a Ti\|Ti-Ru-Ir-Oxides Anode. *Chem. Eng. Process.* **2024**, *196*, 109634.
(54) Nath, H.; Wang, X.; Torrens, R.; Langdon, A. A Novel Perforated Electrode Flow through Cell Design for Chlorine Generation. *J. Appl. Electrochem.* **2011**, *41* (4), 389−395.
(55) Mostafa, E.; Reinsberg, P.; Garcia-Segura, S.; Baltruschat, H. Chlorine Species Evolution during Electrochlorination on Boron-Doped Diamond Anodes: In-Situ Electrogeneration of Cl2, Cl2O and ClO2. *Electrochim. Acta* **2018**, *281*, 831−840.
(56) Khelifa, A.; Moulay, S.; Hannane, F.; Benslimene, S.; Hecini, M. Application of an Experimental Design Method to Study the Performance of Electrochlorination Cells. *Desalination* **2004**, *160* (1), 91−98.
(57) Naderi, M.; Nasseri, S. Optimization of Free Chlorine, Electric and Current Efficiency in an Electrochemical Reactor for Water Disinfection Purposes by RSM. *J. Environ. Health Sci. Eng.* **2020**, *18* (2), 1343−1350.
(58) Waegele, M. M.; Gunathunge, C. M.; Li, J.; Li, X. How Cations Affect the Electric Double Layer and the Rates and Selectivity of Electrocatalytic Processes. *J. Chem. Phys.* **2019**, *151* (16), 160902.
(59) Kribeche, M. E. A.; Zaviska, F.; Brosillon, S.; Heran, M. Water Composition and Electrocatalytic Aspects for Efficient Chlorine Generation. *Electrocatalysis* **2022**, *13* (4), 414−424.
(60) Lei, Y.; Lei, X.; Westerhoff, P.; Zhang, X.; Yang, X. Reactivity of Chlorine Radicals (Cl• and Cl2•-) with Dissolved Organic Matter and the Formation of Chlorinated Byproducts. *Environ. Sci. Technol.* **2021**, *55* (1), 689−699.
(61) Zhang, F.; Sun, Z.; Cui, J. Research on the Mechanism and Reaction Conditions of Electrochemical Preparation of Persulfate in a Split-Cell Reactor Using BDD Anode. *RSC Adv.* **2020**, *10* (56), 33928−33936.
(62) Barazesh, J. M.; Prasse, C.; Sedlak, D. L. Electrochemical Transformation of Trace Organic Contaminants in the Presence of Halide and Carbonate Ions. *Environ. Sci. Technol.* **2016**, *50* (18), 10143−10152.
(63) Kuhn, A. T.; Hamzah, H.; Collins, G. C. S. The Inhibition of the Cathodic Reduction of Hypochlorite by Films Deposited at the Cathode Surface. *J. Chem. Technol. Biotechnol.* **1980**, *30* (1), 423−428.
(64) World Health Organization; WHO. *Guidelines for Drinking-Water Quality*; World Health Organization, 2004; Vol. *1*.
(65) Jolley, R. L.; Brungs, W. A.; Cotruvo, J. A.; Cumming, R. B.; Mattice, J. S.; Jacobs, V. A. *Water Chlorination: Environmental Impact and Health Effects. Volume 4, Book 1. Chemistry and Water Treatment*; Ann Arbor Science Publishers: Ann Arbor, MI, 1983, pp 1−18.
(66) Nagata, J. M.; Valeggia, C. R.; Smith, N. W.; Barg, F. K.; Guidera, M.; Bream, K. D. W. Criticisms of Chlorination: Social Determinants of Drinking Water Beliefs and Practices among the Tz'utujil Maya. *Rev. Panam. Salud Publica* **2011**, *29* (1), 9−16.
(67) Crider, Y.; Sultana, S.; Unicomb, L.; Davis, J.; Luby, S. P.; Pickering, A. J. Can You Taste It? Taste Detection and Acceptability Thresholds for Chlorine Residual in Drinking Water in Dhaka, Bangladesh. *Sci. Total Environ.* **2018**, *613−614*, 840−846.
(68) Hubler, D. K.; Baygents, J. C.; Chaplin, B. P.; Farrell, J. Understanding Chlorite, Chlorate and Perchlorate Formation When Generating Hypochlorite Using Boron Doped Diamond Film Electrodes. *ECS Trans.* **2014**, *58* (35), 21−32.
(69) Neodo, S.; Rosestolato, D.; Ferro, S.; De Battisti, A. On the Electrolysis of Dilute Chloride Solutions: Influence of the Electrode Material on Faradaic Efficiency for Active Chlorine, Chlorate and Perchlorate. *Electrochim. Acta* **2012**, *80*, 282−291.
(70) Otter, P.; Hertel, S.; Ansari, J.; Lara, E.; Cano, R.; Arias, C.; Gregersen, P.; Grischek, T.; Benz, F.; Goldmaier, A.; Alvarez, J. A. Disinfection for Decentralized Wastewater Reuse in Rural Areas through Wetlands and Solar Driven Onsite Chlorination. *Sci. Total Environ.* **2020**, *721*, 137595.
(71) Yi, J.; Ahn, Y.; Hong, M.; Kim, G.-H.; Shabnam, N.; Jeon, B.; Sang, B.-I.; Kim, H. Comparison between OCl–Injection and In Situ Electrochlorination in the Formation of Chlorate and Perchlorate in Seawater. *Appl. Sci.* **2019**, *9* (2), 229.
(72) Jung, Y. J.; Baek, K. W.; Oh, B. S.; Kang, J.-W. An Investigation of the Formation of Chlorate and Perchlorate during Electrolysis Using Pt/Ti Electrodes: The Effects of PH and Reactive Oxygen Species and the Results of Kinetic Studies. *Water Res.* **2010**, *44* (18), 5345−5355.

https://doi.org/10.1021/acssuschemeng.3c07066
ACS Sustainable Chem. Eng. 2024, 12, 3130−3141

(73) Bakheet, B.; Prodanovic, V.; Deletic, A.; McCarthy, D. Effective Treatment of Greywater via Green Wall Biofiltration and Electrochemical Disinfection. *Water Res.* **2020**, *185*, 116228.
(74) Hand, S.; Cusick, R. D. Electrochemical Disinfection in Water and Wastewater Treatment: Identifying Impacts of Water Quality and Operating Conditions on Performance. *Environ. Sci. Technol.* **2021**, *55* (6), 3470−3482.
(75) Kerwick, M. I.; Reddy, S. M.; Chamberlain, A. H. L.; Holt, D. M. Electrochemical Disinfection, an Environmentally Acceptable Method of Drinking Water Disinfection? *Electrochim. Acta* **2005**, *50* (25−26), 5270−5277.
(76) Saha, J.; Gupta, S. K. A Novel Electro-Chlorinator Using Low Cost Graphite Electrode for Drinking Water Disinfection. *Ionics* **2017**, *23* (7), 1903−1913.
(77) Shih, Y.-J.; Su, C.-C.; Lu, M.-C.; Huang, C. P. The Electrodeless Preparation of M (M = Pt, Pd, Ru, Cu) NiCo Oxide/Graphite Electrodes for the Electrochemical Inactivation of Escherichia Coli. *Sustainable. Environ. Res.* **2016**, *26* (1), 1−13.
(78) Kuhn, A. T.; Mortimer, C. J. The Efficiency of Chlorine Evolution in Dilute Brines on Ruthenium Dioxide Electrodes. *J. Appl. Electrochem.* **1972**, *2* (4), 283−287.
(79) Otter, P.; Sattler, W.; Grischek, T.; Jaskolski, M.; Mey, E.; Ulmer, N.; Grossmann, P.; Matthias, F.; Malakar, P.; Goldmaier, A.; Benz, F.; Ndumwa, C. Economic Evaluation of Water Supply Systems Operated with Solar-Driven Electro-Chlorination in Rural Regions in Nepal, Egypt and Tanzania. *Water Res.* **2020**, *187*, 116384.
(80) Amdoun, R.; Khelifi, L.; Khelifi-Slaoui, M.; Amroune, S.; Asch, M.; Assaf-Ducrocq, C.; Gontier, E. The Desirability Optimization Methodology; a Tool to Predict Two Antagonist Responses in Biotechnological Systems: Case of Biomass Growth and Hyoscyamine Content in Elicited Datura Starmonium Hairy Roots. *Iran. J. Biotechnol.* **2018**, *16* (1), 11−19.
(81) Kuhn, A. T.; Lartey, R. B. Electrolytic Generation "In-Situ" of Sodium Hypochlorite. *Chem. Ing. Tech.* **1975**, *47* (4), 129−135.
(82) Kearney, D.; Bejan, D.; Bunce, N. J. The Use of Ebonex Electrodes for the Electrochemical Removal of Nitrate Ion from Water. *Can. J. Chem.* **2012**, *90* (8), 666−674.

https://doi.org/10.1021/acssuschemeng.3c07066
ACS Sustainable Chem. Eng. 2024, 12, 3130−3141